AIAA Meeting Papers on Disc, 1996, pp. 521-533
A9635137, AIAA Paper 96-3425

Higher-order analytic solutions for critical cases of ballistic entry

Nguyen X. Vinh
Michigan Univ., Ann Arbor

L. de-O. Ferreira
Michigan Univ., Ann Arbor

Eun-Kyou Kim
Michigan Univ., Ann Arbor

Donald T. Greenwood
Michigan Univ., Ann Arbor

AIAA Atmospheric Flight Mechanics Conference, San Diego, CA, July 29-31, 1996, Technical Papers (A96-35084 09-08), Reston, VA, American Institute of Aeronautics and Astronautics, 1996

A new set of higher-order analytic solutions is introduced for the critical cases of: ballistic skip trajectories with initial speed greater than the circular orbital speed (supercircular case); shallow ballistic entry with entry speed less than the circular orbital speed (subcircular case); and shallow ballistic entry from low circular orbits (circular case). Both noncircular cases admit the same set of analytic solutions, except that the supercircular case involves the regular error function of a real argument, whereas in the subcircular case the solution depends on error functions of an imaginary argument. Unlike previously obtained solutions, neither case now exhibits singularities in the flight path angle. For the circular case, a totally independent set of parametric expressions is obtained. In comparison with the numerical integration of the equations of motion, the analytic solutions exhibit a high degree of accuracy, representing a clear improvement over equivalent solutions currently available in the literature. (Author)

96-3425

A96-35137 AIAA-96-3425-CP

HIGHER-ORDER ANALYTIC SOLUTIONS FOR CRITICAL CASES OF BALLISTIC ENTRY

Nguyen X. Vinh,* L. de-Olivé Ferreira,† Eun-Kyou Kim,§ Donald T. Greenwood‡
Dept. of Aerospace Engineering, The University of Michigan
Ann Arbor, MI 48109-2118

Abstract

A new set of higher-order analytic solutions is introduced for the critical cases of: (a) ballistic skip trajectories with initial speed greater than the circular orbital speed (supercircular case); (b) shallow ballistic entry with entry speed less than the circular orbital speed (subcircular case); and (c) shallow ballistic entry from low circular orbits (circular case). Both non-circular cases admit the same set of analytic solutions, except that the supercircular case involves the regular error function of real argument, whereas in the subcircular case the solution depends on error functions of imaginary argument. Unlike previously obtained solutions, neither case now exhibits singularities in the flight path angle. For the circular case, a totally independent set of parametric expressions is obtained. In comparison with the numerical integration of the equations of motion, the analytic solutions exhibit a high degree of accuracy, representing a clear improvement over equivalent solutions currently available in the literature.

Nomenclature

B = small parameter specifying entry altitude and physical characteristics of vehicle
$\overline{B}$ = B/E^*
C_D, C_L = coefficients of drag and lift, respectively
C_{D_0} = zero-lift drag coefficient
c = dimensionless flight path angle at entry
D = drag
E^* = maximum lift-to-drag ratio
g = magnitude of the acceleration due to gravity
h = dimensionless altitude from the reference level
K = induced drag factor
k = auxiliary dimensionless parameter in the analysis of ballistic entry
L = lift
m = vehicle's mass
r = radial distance from planet's center
S = vehicle's characteristic area
t = time
u = dimensionless speed in terms of the kinetic energy
V = speed along the trajectory
x = initial dimensionless flight path angle (non-circular cases)
y = dimensionless altitude (density) variable
z = auxiliary dimensionless variable in the computation of the altitude

- Greek letters:

α = parameter defining trajectory type
β = inverse scale height
γ = flight path angle
δ = $2(1-\alpha)$
η = $\overline{B}/\sqrt{\beta r_0}$
θ = range angle
λ = normalized lift coefficient
ν = dimensionless speed
ρ = atmospheric density
τ = transformed range angle
ϕ = dimensionless flight path angle
χ = transformed longitude

- Subscripts:

e : condition at entry
0 : reference trajectory

Introduction

After Chapman's classic first-order analytic solution,[1] Loh,[2] Yaroshevskii,[3] and Longuski and Vinh,[4] working independently, proposed different sets of second-order solutions for planetary entry trajectories, seeking greater accuracy for guidance purposes. But all those solutions left something to be desired. Loh's integration of the equations of motion was heuristic, introducing a step which finds no mathematical justification. On the other hand, inspired by Chapman's ideas, Yaroshevskii's formulation is plagued by a strong singularity in the flight path angle, which is dealt with in a somewhat artificial way. Following a similar path, Longuski and Vinh integrated a system of simplified equations of motion, both numerically and analytically. Their work yields good results to within the validity of the simplifications made, except in the critical case of shallow entry.

In physical applications, ballistic missiles typically reenter the dense atmosphere from subcircular orbital

---

* Professor of Aerospace Engineering. Member, AIAA.

† Research fellow. Member, AIAA.

§ Research fellow.

‡ Professor Emeritus of Aerospace Engineering. Associate Fellow, AIAA.

speeds (with the entry angle small in magnitude). Also, the abort of ascending flights of space vehicles is followed by an entry-like trajectory starting at subcircular speed. Thus, the ability to predict these types of trajectories with accuracy and rapidity is of fundamental importance in both theory and practice. Furthermore, the current interest in aeroassist technology obviously necessitates good determination of skip trajectories. In addition, low-eccentricity, low-altitude orbits typically graze the outer layers of the atmosphere at approximately the circular orbital speed. That is the case of several classes of satellites which, upon reaching the end of their useful lifetime, normally reenter the atmosphere somewhere along the grazing portion of their orbits.

In brief, a clear need exists for good analytic solutions involving critical entry trajectories. This paper addresses such a problem, giving sequence to work started with Ref. 5. To that end, the equations of motion are normalized through a set of Chapman-type nondimensional variables, being subsequently put in a form suitable for integration by analytic continuation. Unlike previous works[2] (where approximate differential relations between the main variables were integrated directly), here we manage to integrate the equations of motion in terms of the longitude. This enables the researcher to predict altitude, speed, flight path angle, and deceleration at any point along the trajectory as functions of the entry conditions and the current position only, instead of having to infer the position from cross-plots. The resulting analytic solutions have been found to be remarkably accurate and of fast computation for any non-thrusting, non-lifting aerospace vehicle, in any planetary atmosphere, through practically the entire range of hypersonic velocities. As a matter of fact, for the Earth's atmosphere, even at low supersonic speeds (Mach 1.6), the analytic expressions herein predict speed, altitude, and deceleration due to atmospheric drag with a level of accuracy never before achieved. These expressions thus lend themselves well to programming on on-board computers for in-flight propagation of the nominal trajectory. They are also well suited for the generation, e.g., of reference trajectories for mission planning and the stability analysis of entry trajectories.

The Dimensionless Equations of Motion

For planar entry of a non-thrusting, lifting vehicle into a non-rotating spherical planetary atmosphere, we have the equations

$$\frac{dr}{dt} = V\sin\gamma \tag{1.a}$$

$$r\frac{d\theta}{dt} = V\cos\gamma \tag{1.b}$$

$$\frac{dV}{dt} = -\frac{D}{m} - g\sin\gamma \tag{1.c}$$

$$V\frac{d\gamma}{dt} = \frac{L}{m} - \left(g - \frac{V^2}{r}\right)\cos\gamma \tag{1.d}$$

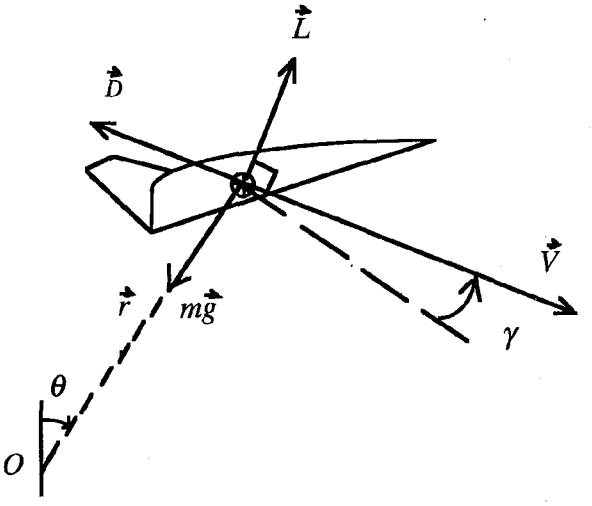

Figure 1 - Nomenclature

Using the initial altitude as a reference, we consider a central Newtonian gravitational attraction and an exponential atmosphere, that is,

$$\frac{g}{g_0} = \frac{r_0^2}{r^2} \tag{2}$$

and

$$\frac{\rho}{\rho_0} = e^{-\beta(r-r_0)} \tag{3}$$

For the lift-drag relationship we use the standard parabolic polar

$$C_D = C_{D_0} + KC_L^2 \tag{4}$$

with constant C_{D_0} and K for hypersonic flow. The altitude and speed variables are nondimensionalized through the following definitions:

$$h = \frac{r - r_0}{r_0} \tag{5}$$

$$u = \frac{V^2}{g_0 r_0} \tag{6}$$

Then we have the equations of motion, with the time eliminated in favor of the range angle:

$$\frac{dh}{d\theta} = (1+h)\tan\gamma \tag{7a}$$

$$\frac{du}{d\theta} = -\frac{B(1+h)(1+\lambda^2)ue^{-\beta r_0 h}}{E^* \cos\gamma} - \frac{2}{(1+h)}\tan\gamma \tag{7b}$$

$$\frac{d\gamma}{d\theta} = \frac{B(1+h)\lambda e^{-\beta r_0 h}}{\cos\gamma} - \frac{1}{u(1+h)} + 1 \tag{7c}$$

where E^* is the maximum lift-to-drag ratio and B is a small parameter specifying the entry altitude and physical characteristics of the vehicle.

$$E^* = \frac{1}{2\sqrt{KC_{D_0}}} \tag{8}$$

$$B = \frac{\rho_0 S r_0}{2m}\sqrt{\frac{C_{D_0}}{K}} \tag{9}$$

The system (7) constitutes the exact equations for re-entry, even with lift modulation. The lift control here is the normalized lift coefficient

$$\lambda = \frac{C_L}{\sqrt{C_{D_0}/K}} \tag{10}$$

which is defined such that, when $\lambda = 1$, the flight is at maximum lift-to-drag ratio. Analytic solutions can be obtained for constant λ, with the limiting case of $\lambda = 0$ for ballistic entry. The equations are integrated from the initial entry point at $\theta = 0$ with $h = 0$, $u = u_e$, $\gamma = \gamma_e$. The atmosphere is here specified by the so-called Chapman's parameter βr_0, while E^* is the performance characteristic of the vehicle. The other physical characteristics of the vehicle, such as its mass and size are contained in the dimensionless parameter B, which also serves as an indication of the entry altitude.

To perform the integration, we introduce new dimensionless variables with y for altitude, v for speed and ϕ for flight path angle, such that

$$y = e^{-\beta r_0 h} = \frac{\rho}{\rho_0} \tag{11}$$

$$v = \frac{1}{\eta}\ln\frac{V_e^2}{V^2} \tag{12}$$

$$\phi = -\sqrt{\beta r_0}\sin\gamma \tag{13}$$

where V_e is the entry speed and η is a small constant defined as

$$\eta = \frac{B}{E^*\sqrt{\beta r_0}} = \frac{\rho_0 S C_{D_0}}{m}\sqrt{\frac{r_0}{\beta}} \tag{14}$$

For a typical entry vehicle at 100 km in the Earth's atmosphere, η is of the order of 10^{-4}. In addition, the new variables defined above are such that, at entry, we always have $y(0) = 1$ and $v(0) = 0$. With these definitions, system (7) is transformed into

$$\frac{dy}{d\tau} = \frac{(1+h)}{\cos\gamma} y\phi \tag{15a}$$

$$\frac{dv}{d\tau} = \frac{(1+h)}{\cos\gamma}(1+\lambda^2)y - \frac{1}{(1+h)\cos\gamma} k\alpha\phi e^{\eta v} \tag{15b}$$

$$\frac{d\phi}{d\tau} = -(1+h)B\lambda y + \frac{\cos\gamma}{(1+h)}\alpha e^{\eta v} - \cos\gamma \tag{15c}$$

where $\tau = \sqrt{\beta r_0}\,\theta$ is the new independent variable and

$$k = \frac{2E^*}{\sqrt{\beta r_0 B}} \tag{16}$$

$$\alpha = \frac{g_0 r_0}{V_e^2} \tag{17}$$

The system (15) is the exact system, but the selection of the dimensionless variables, combined with the fact that, for entry trajectories, $\cos\gamma \approx 1$, $1+h \approx 1$, leads to the simpler system

$$\frac{dy}{d\tau} = y\phi \tag{18a}$$

$$\frac{dv}{d\tau} = (1+\lambda^2)y - k\alpha\phi e^{\eta v} \tag{18b}$$

$$\frac{d\phi}{d\tau} = -B\lambda y + \alpha e^{\eta v} - 1 \tag{18c}$$

Extensive numerical integration performed for several cases of entry trajectories has shown that the solutions to (18) are nearly the same as those obtained from (15).

In summary, system (18) comprises the dimensionless equations of motion for re-entry, with y being the density ratio (used as the altitude variable), v the speed variable and ϕ the flight path angle variable, while τ is proportional to the distance traveled. At $\tau = 0$, we always have $y(0) = 1$ and $v(0) = 0$. The initial entry speed is now specified by the dimensionless parameter α, with $\alpha = 1$ for circular entry and $\alpha = 0.5$ for parabolic entry. The planetary atmosphere is specified by Chapman's characteristic parameter in the form of the product βr_0, with the value $\beta r_0 \approx 900$ for the Earth's atmosphere. The vehicle physical characteristics are

specified by the maximum lift-to-drag ratio E^* and the dimensionless parameter B, which also includes the effective entry altitude. The number of physical parameters required for the analysis has thus been reduced to a minimum. In order to generate the trajectory, it suffices to select an entry angle γ_e (with which the initial value $\phi_e = -\sqrt{\beta r_0}\sin\gamma_e$ is evaluated) and to specify the flight program in terms of λ, the coefficient of lift.

The Non-Circular Cases

In this section we analyze both the case of ballistic skip with an initial speed greater than the local circular speed and the case of ballistic entry from a subcircular speed. — As ballistic trajectories are generally characterized by the absence of aerodynamic lift, that is, a zero normalized lift coefficient ($\lambda = 0$), system (18) is particularized to

$$\frac{dy}{d\tau} = y\phi \tag{19a}$$

$$\frac{dv}{d\tau} = y - k\alpha\phi e^{\eta v} \tag{19b}$$

$$\frac{d\phi}{d\tau} = \alpha e^{\eta v} - 1 \tag{19c}$$

with initial conditions at $\tau = 0$

$$y(0) = 1, \quad v(0) = 0, \quad \phi(0) = c \tag{20}$$

In addition to the value $c = -\sqrt{\beta r_0}\sin\gamma_e > 0$ for the entry angle, the entry speed is specified by selecting a value for α. The vehicle physical characteristics and the effective entry altitude are contained in the two parameters k and η. For ballistic trajectories, since $\beta r_0 \approx 900$ is known for the Earth's atmosphere, it suffices to specify

$$\overline{B} = \frac{B}{E^*} = \frac{\rho_0 S C_{D_0} r_0}{m} \tag{21}$$

to replace both k and η. Therefore, a ballistic trajectory is governed by the initial speed, the initial angle and the factor $\overline{B}$ as defined in Eq. (21).

Even though the ballistic entry mode at subcircular speed and moderate entry angle has been extensively studied in the past, with accurate solutions having been obtained,[4] a new, improved set of solutions is derived here. For aeroassisted orbital transfer and planetary aerocapture, we may use the ballistic mode as well. With supercircular initial speed and a small initial angle, the vehicle will skip out and the accurate prediction of the exit speed and exit angle using explicit analytic expressions is of obvious interest to mission planning. Furthermore, if, in addition to being accurate, such expressions are also fast enough computationally to become competitive when compared to the numerical integration of the exact equations of motion, these analytic expressions can then be used for guidance purposes advantageously.

It will become apparent in the following derivation that both the ballistic skip and the actual ballistic entry admit essentially the same set of analytic solutions, with the only notable difference residing in the evaluation of the speed. As we shall see, in the supercircular case, the speed is given by a combination of error functions of real arguments. On the other hand, the speed in the subcircular case depends on error functions of imaginary arguments.

Higher-order analytic solutions are obtained by observing that η is a small parameter, of the order of 10^{-4}. Hence, we seek solutions of the form

$$\begin{aligned} y &= y_0 + \eta y_1 + \eta^2 y_2 + \ldots \\ v &= v_0 + \eta v_1 + \eta^2 v_2 + \ldots \\ \phi &= \phi_0 + \eta\phi_1 + \eta^2\phi_2 + \ldots \end{aligned} \tag{22}$$

with initial conditions

$$y_0(0) = 1, \quad v_0(0) = 0, \quad \phi_0(0) = c \tag{23}$$

and

$$y_i(0) = 0, \quad v_i(0) = 0, \quad \phi_i(0) = 0, \quad i = 1,2,\ldots \tag{24}$$

Substituting (22) into (19) and equating terms of like powers in η, the following systems of various orders are obtained:

$$\begin{aligned} \frac{dy_0}{d\tau} &= y_0\phi_0 \\ \frac{dv_0}{d\tau} &= y_0 - k\alpha\phi_0 \\ \frac{d\phi_0}{d\tau} &= -(1-\alpha) \end{aligned} \tag{25}$$

$$\begin{aligned} \frac{dy_1}{d\tau} &= y_0\phi_1 + y_1\phi_0 \\ \frac{dv_1}{d\tau} &= y_1 - k\alpha(\phi_0 v_0 + \phi_1) \\ \frac{d\phi_1}{d\tau} &= \alpha v_0 \end{aligned} \tag{26}$$

$$\begin{aligned} \frac{dy_2}{d\tau} &= y_0\phi_2 + y_1\phi_1 + y_2\phi_0 \\ \frac{dv_2}{d\tau} &= y_2 - k\alpha\left(\phi_0 v_1 + \frac{1}{2}\phi_0 v_0^2 + \phi_1 v_0 + \phi_2\right) \\ \frac{d\phi_2}{d\tau} &= \alpha\left(v_1 + \frac{1}{2}v_0^2\right) \end{aligned} \tag{27}$$

Since the solution for ϕ_0 is linear in τ, it is convenient to use this function as the new independent variable. For ease of notation, let

$$x = \phi_0 \tag{28}$$

$$\delta = 2(1-\alpha) \tag{29}$$

Notice that, in the supercircular case, $\alpha < 1$, implying $\delta > 0$. In the subcircular case, however, $\alpha > 1$ and $\delta < 0$.

Introducing the above definitions into system (25), the equations for the first-order solution become

$$\begin{aligned} \frac{dy_0}{dx} &= -\frac{2}{\delta} y_0 x \\ \frac{dv_0}{dx} &= -\frac{2}{\delta} y_0 + \frac{2k\alpha}{\delta} x \end{aligned} \tag{30}$$

With the initial value of $x(0) = c$, the solution is readily obtained as

$$y_0 = \exp\left(\frac{c^2 - x^2}{\delta}\right) \tag{31}$$

$$\begin{aligned} v_0 = &-\frac{k\alpha}{\delta}\left(c^2 - x^2\right) \\ &+ \sqrt{\frac{\pi}{\delta}} \exp\left(\frac{c^2}{\delta}\right)\left[\operatorname{erf}\left(\frac{c}{\sqrt{\delta}}\right) - \operatorname{erf}\left(\frac{x}{\sqrt{\delta}}\right)\right] \end{aligned} \tag{32}$$

where the error function is defined as

$$\operatorname{erf}(z) = \frac{2}{\sqrt{\pi}} \int_0^z e^{-\zeta^2} d\zeta \tag{33}$$

and z is a complex variable. — Evidently, with $\delta > 0$, all the square roots contained in Eq. (32) are real, and the error functions therein are of the ordinary type, in the supercircular case. On the other hand, in the subcircular case, with $\delta < 0$, the square roots in Eq. (32) are imaginary, so the arguments of the error functions are now imaginary. To perform the evaluation of Eq. (32) when $\delta < 0$, we resort to a series approximation for the complex error function as listed in Ref. 6 and first published by Salzer.[7] Upon applying that series approximation to the problem of ballistic entry (and using the dimensionless variables defined above), the analytic expression for the speed during ballistic entry becomes

$$\begin{aligned} v_0 = &-\frac{k\alpha}{\delta}\left(c^2 - x^2\right) + \frac{1}{\delta\sqrt{\pi}} \exp\left(\frac{c^2}{\delta}\right) \\ &\times \left\{(c-x) + 2\sqrt{-\delta} \sum_{n=1}^{\infty} \left(\frac{1}{n e^{n^2/4}}\right)\left[\sinh\left(\frac{nc}{\sqrt{-\delta}}\right) - \sinh\left(\frac{nx}{\sqrt{-\delta}}\right)\right]\right\} \end{aligned} \tag{34}$$

Before we proceed, a few remarks concerning Eq. (34) are in order. Analytic determination of the radius of convergence of the series has proven to be a rather difficult task. Nevertheless, it has been found that, to within the double-precision arithmetic available on present-day computers and depending on the entry angle c, maximum accuracy will be obtained by taking between 25 and 50 terms in the series, with 25 corresponding to small entry angles ($|\gamma_e| \le 10°$). In fact, from a numerical viewpoint, by utilizing a refined increment of the independent variable x, good results will be obtained with 25 terms in any case. This seems to be in agreement with Salzer's recommendation. By means of error analysis, he concluded that 24 terms should lead to maximum accuracy.

Clearly, an alternate expression for v_0 in the subcircular case can be obtained via term-by-term integration of the series expansion of the exponential function in Eq. (33). The results match those from Eq. (34) exactly. But, for the same degree of accuracy and same value of c, the alternate expression typically requires three to six times as many terms as Eq. (34), rendering the computation excessively slow.

Now, from the last equation in system (25), ϕ_0 is related to the distance traveled by

$$\phi_0 = -\frac{\delta}{2}\tau + c \tag{35}$$

Although ϕ_0 is the first-order solution for the flight path angle, we use it in the higher-order solution simply as the independent variable, which is monotonically varying, by putting $x = \phi_0$, to rewrite systems (26) and (27) as

$$\frac{d\phi_1}{dx} = -\frac{2\alpha}{\delta} v_0 \tag{36a}$$

$$\frac{dy_1}{dx} = -\frac{2}{\delta} y_0 \phi_1 - \frac{2}{\delta} y_1 x \tag{36b}$$

$$\frac{dv_1}{dx} = -\frac{2}{\delta} y_1 + \frac{2k\alpha}{\delta} \phi_1 + \frac{2k\alpha}{\delta} v_0 x \tag{36c}$$

$$\frac{d\phi_2}{dx} = -\frac{2\alpha}{\delta} v_1 - \frac{\alpha}{\delta} v_0^2 \tag{37a}$$

$$\frac{dy_2}{dx} = -\frac{2}{\delta} y_0 \phi_2 - \frac{2}{\delta} y_1 \phi_1 - \frac{2}{\delta} y_2 x \tag{37b}$$

$$\begin{aligned} \frac{dv_2}{dx} = &-\frac{2}{\delta} y_2 + \frac{2k\alpha}{\delta} \phi_2 + \frac{2k\alpha}{\delta} \phi_1 v_0 \\ &+ \frac{2k\alpha}{\delta} v_1 x + \frac{k\alpha}{\delta} v_0^2 x \end{aligned} \tag{37c}$$

The second-order solutions are obtained by integrating system (36) with null initial values for all the variables. Then, substituting the first- and second-order solutions into system (37), the same process can be used to obtain third-order solutions, and so on.

First, using the solution for v_0 in Eq. (36a), $\phi_1(x)$ is obtained by quadrature. It has been found that by direct integration by parts along with an efficient use of the existing differential relations, one can always cast the integration of a long expression into some simple integrals. For example:

$$\begin{aligned}\phi_1 &= -\frac{2\alpha}{\delta}\int v_0\,dx \\ &= -\frac{2\alpha}{\delta}v_0x + \frac{2\alpha}{\delta}\int x\,dv_0 \\ &= -\frac{2\alpha}{\delta}v_0x + \frac{2\alpha}{\delta}\int x\left(-\frac{2}{\delta}y_0 + \frac{2k\alpha}{\delta}x\right)dx \\ &= -\frac{2\alpha}{\delta}v_0x + \frac{4k\alpha^2}{3\delta^2}x^3 + \frac{2\alpha}{\delta}\int dy_0 \\ &= -\frac{2\alpha}{\delta}v_0x + \frac{4k\alpha^2}{3\delta^2}x^3 + \frac{2\alpha}{\delta}y_0 + C\end{aligned} \tag{38}$$

where C is a constant. Then, with the initial condition $\phi_1(0) = 0$,

$$\phi_1 = \frac{2\alpha}{\delta}\left(y_0 - v_0x - 1\right) - \frac{4k\alpha^2}{3\delta^2}\left(c^3 - x^3\right) \tag{39}$$

Next, observing that the homogeneous equation for y_1 (and later on, for y_2, y_3, ...) is of the same form as the equation for y_0, we put

$$y_i = y_0 z_i, \quad i = 1,2,\ldots \tag{40}$$

Then, Eq. (36b) for y_1 becomes

$$\frac{dz_1}{dx} = -\frac{2}{\delta}\phi_1 \tag{41}$$

with initial condition $z_1(0) = 0$. The remark made above about integration by parts with successive transformations of the integrals involved applies here as well. The final result for y_1, after using this procedure to obtain z_1, is

$$\begin{aligned}y_1 = &-\frac{2\alpha}{\delta^2}y_0x\left[y_0 - v_0x - 1 - \frac{4k\alpha}{3\delta}\left(c^3 - x^3\right)\right] \\ &-\frac{k\alpha^2}{\delta^2}y_0\left[\frac{1}{\delta}\left(c^4 - x^4\right) - \left(c^2 - x^2\right)\right] \\ &+\frac{\alpha}{\delta}y_0\left[v_0 - \frac{2}{\delta}(c - x)\right]\end{aligned} \tag{42}$$

Substituting v_0, ϕ_1 and y_1 in Eq. (36c), we obtain v_1 by quadrature, using the same technique of integration by parts.

$$\begin{aligned}v_1 = &-\frac{2\alpha}{\delta^2}y_0\left[y_0 - v_0x - 1 - \frac{4k\alpha}{3\delta}\left(c^3 - x^3\right)\right] \\ &+\frac{4k\alpha^2}{\delta^2}x\left[y_0 - v_0x - 1 - \frac{2k\alpha}{3\delta}\left(c^3 - x^3\right)\right] \\ &+\frac{2\alpha}{\delta^2}y_0\left[\frac{k\alpha}{2\delta}x^3 - \frac{k(4-\alpha)}{4}x + 1\right] \\ &-\frac{2\alpha}{\delta^2}\left[\frac{k\alpha}{2\delta}c^3 - \frac{k(4-\alpha)}{4}c + 1\right] \\ &-\frac{2\alpha}{\delta}\left[\frac{k\alpha}{2\delta^2}c^4 - \frac{k\alpha}{2\delta}c^2 + \frac{c}{\delta} + \frac{k(4-\alpha)}{8}\right] \\ &\times\left[v_0 + \frac{k\alpha}{\delta}\left(c^2 - x^2\right)\right] \\ &+\frac{\alpha}{\delta}v_0^2 + \frac{k\alpha}{\delta}v_0x^2 + \frac{k^2\alpha^2}{2\delta^2}\left(c^4 - x^4\right)\end{aligned} \tag{43}$$

It should be noted that these second-order solutions are valid for both the cases of super- and subcircular entry. Particularization to either case requires only that the appropriate solution for v_0 be used in the second-order expressions.

It is also of interest to assess the deceleration due to aerodynamic drag when planning any entry-like trajectory. This deceleration is given by

$$\frac{a}{g} = -\frac{1}{g}\frac{dV}{dt} = \frac{\rho S C_D V^2}{2mg} \tag{44}$$

With $g \approx g_0$ and using the dimensionless variables previously selected, the above expression becomes

$$\frac{a}{g_0} = \frac{\overline{B}}{2\alpha}ye^{-\eta v} = \frac{\overline{B}}{2}yu \tag{45}$$

It should now be apparent that, except for the computation of v_0, either by Eq. (32) or by Eq. (34), the difference between super- or subcircular entry has no major bearing on the solution process, with the same set of analytic expressions resulting for altitude, flight path angle and speed.

To test the accuracy of the solution, we first consider the ballistic skip trajectory of a vehicle with $\overline{B} = B/E^* = 0.005/0.75$. Again, we emphasize the fact that it is sufficient to provide a value for $\overline{B}$ as defined in Eq. (21). Figures 2 and 3 display the results for an entry angle of $\gamma_e = -3°$ with various values of entry speed, while Figs. 4 and 5 have the results for parabolic entry

($u_e = 2$) at several entry angles. Notice that $u_e = 1.733$ corresponds to the entry speed for the return from a geosynchronous orbit. When u_e tends to the circular speed, the accuracy decreases, necessitating a new analytic solution. In all figures the solid lines correspond to the numerical solution, while the dashed and dotted lines represent the analytic solutions of various orders.

Firstly, we note that the figures display the correct behavior corresponding to a skip trajectory. Initially, the incoming vehicle dips into the upper layers of the atmosphere. Then, by interacting with the atmosphere, the vehicle negotiates a change in its velocity vector, both in magnitude and direction (characterized by a decrease in the speed and a reversal of sign of the flight path angle). The vehicle eventually skips out of the atmosphere at a speed less than the initial speed. During the maneuver, as the altitude decreases, the atmospheric density increases, inducing an ever greater aerodynamic drag, which translates into an increasing deceleration, until the vehicle hits the absolute lowest point on its trajectory, with the peak deceleration occurring shortly before that point. From then on, as the flight path angle becomes positive and the vehicle turns up, on its way out of the atmosphere, the density, the drag, and the deceleration continuously decrease, vanishing as the vehicle leaves the atmosphere.

From the plots, it can readily be seen that the analytic solutions closely follow the numerical results, with the second-order solution consistently yielding better approximations than the first-order solution and nearly overlapping with the numerical curves. For a given value of the entry angle (say, $\gamma_e = -3°$), the higher the entry speed, the closer the analytic solutions will match the numerical solution. As lower values of the entry speed are chosen, the agreement between analytic and numerical becomes less and less satisfactory until, for entry speeds below 1.1 times the circular orbital speed, the present set of solutions no longer yields reliable predictions. Furthermore, it has been found that, in order to obtain acceptable results corresponding to such low entry speeds, the entry angle must be tightly controlled, remaining within the $-2° \le \gamma_e \le 0°$ range. On the other hand, for a given value of the entry speed (say, the parabolic entry speed, $u_e = 2$), by increasing the absolute value of the entry angle, some accuracy is lost, as the small angle hypothesis is violated. Again, the best results will be obtained by remaining within the range of entry angles mentioned above. We emphasize that the solutions derived up to this point contain no singularity in the flight path angle, which allows the propagation of shallow entry trajectories. They do, however, embody a discontinuity in the entry speed, corresponding to the case of entry from circular orbital speed, for which a totally different set of analytic solutions will be required.

Next, we study the accuracy of the solutions so far obtained when applied to the case of effective entry, that is, the subcircular case. To that end, refer to Figs. 6-8.

These plots reflect a typical Earth re-entry maneuver, injected at $u_e = 0.5$ ($\approx$ Mach 16.3), corresponding to $V/V_c \approx 0.7$. As indicated by the plot of altitude versus dimensionless speed, the vehicle initially plummets steeply into the atmosphere at high speed, covering about half the total altitude range ($|\Delta h| = 0.008$, i.e., altitude variation $\approx$ 51.8 km). By then, the vehicle is deep enough in the atmosphere for the density to become a relevant factor, inducing a sensible increase in aerodynamic drag. The deceleration is now large (reaching a peak at approximately $V/V_c = 0.4$, $h = -0.011$, altitude $\approx$ 28.7 km), so, for the remainder of the trajectory, the altitude varies much more slowly, until the entry phase is completed at about $h = -0.012$, i.e., altitude $\approx$ 22.3 km, and a speed of $u_f = 0.005$ ($V/V_c = 0.07 \approx$ Mach 1.6). The flight path angle initially decreases steeply at high altitude. Then, through the largest portion of the deceleration phase, γ remains nearly constant. Finally, towards the end of the maneuver it begins to decrease fast again. The behavior of the trajectory can be explained by the fact that the entry point at subcircular speed and small entry angle is nearly the apogee of a highly eccentric elliptic orbit and, as such, at the beginning, the radial distance undergoes a fast decrease.

As in the supercircular case, here too it can be seen that, along the entire trajectory, the second-order solution gives much better approximation than the first-order, actually overlapping with the numerical solution through the first half of the trajectory. The accuracy is good. For instance, at the end of the entry phase, the second-order prediction of altitude misses the exact value by 3.7% only. In fact, the analytic predictions of altitude, speed, and deceleration are very accurate. The predictions of the flight path angle are a little less satisfactory, but still within acceptable boundaries. Unlike the supercircular case, now the larger the $|\gamma_e|$, the greater the accuracy.

In general, the equations of motion for each new, higher order depend on the solutions for ϕ, y, and ν of all lower orders. Such being the case, by efficiently exploiting differential relationships extracted from the lower-order equations of motion, those for each new order can be ultimately re-cast in terms of the first-order solution, thus enabling the interested researcher to seek higher-order solutions as needed.

The Circular Case

When the entry is injected at a nominal circular speed, $u_e = 1$, $\alpha = 1$. The systems (25), (26) and (27) then become, respectively,

$$\frac{dy_0}{d\tau} = y_0 \phi_0 \tag{46a}$$

$$\frac{d\nu_0}{d\tau} = y_0 - k\phi_0 \tag{46b}$$

$$\frac{d\phi_0}{d\tau} = 0 \tag{46c}$$

$$\frac{dy_1}{d\tau} = y_0\phi_1 + y_1\phi_0 \tag{47a}$$

$$\frac{dv_1}{d\tau} = y_1 - k\left(\phi_0 v_0 + \phi_1\right) \tag{47b}$$

$$\frac{d\phi_1}{d\tau} = v_0 \tag{47c}$$

$$\frac{dy_2}{d\tau} = y_0\phi_2 + y_1\phi_1 + y_2\phi_0 \tag{48a}$$

$$\frac{dv_2}{d\tau} = y_2 - k\left(\phi_0 v_1 + \frac{1}{2}\phi_0 {v_0}^2 + \phi_1 v_0 + \phi_2\right) \tag{48b}$$

$$\frac{d\phi_2}{d\tau} = v_1 + \frac{1}{2}{v_0}^2 \tag{48c}$$

From (46c), it is evident that, in the circular case, ϕ_0 is a constant,

$$\phi_0 = c \tag{49}$$

So, to obtain the complete first-order solution it is only necessary to integrate the equations for y_0 and v_0. It is convenient to put

$$\chi = c\tau = c\sqrt{\beta r_0}\,\theta \tag{50}$$

where χ is essentially the range angle and has no connection with the variable x used in the derivation of the solutions for the non-circular cases. Notice that χ is a monotonically increasing variable, with zero initial value. Then,

$$\begin{aligned} \frac{dy_0}{d\chi} &= y_0 \\ \frac{dv_0}{d\chi} &= \frac{1}{c}y_0 - k \end{aligned} \tag{51}$$

The integration of these is immediate and gives

$$y_0 = e^{\chi} \tag{52a}$$

$$v_0 = \frac{1}{c}\left(y_0 - 1\right) - k\chi \tag{52b}$$

With the variable χ, the equations for y_1 and y_2 become, respectively,

$$\frac{dy_1}{d\chi} = y_1 + \frac{1}{c}y_0\phi_1 \tag{53}$$

$$\frac{dy_2}{d\chi} = y_2 + \frac{1}{c}y_0\phi_2 + \frac{1}{c}y_1\phi_1 \tag{54}$$

Before attempting to integrate either one, however, it is convenient to once more make the transformation $y_i = y_0 z_i, i = 1,2,\ldots$, to obtain

$$\frac{dz_1}{d\chi} = \frac{1}{c}\phi_1 \tag{55}$$

and

$$\frac{dz_2}{d\chi} = \frac{1}{c}\phi_2 + \frac{1}{c}z_1\phi_1 \tag{56}$$

thus reducing the integration of the altitude variables to a series of quadratures. In addition, since $y_0 = e^{\chi}$, $dy_0 = y_0 d\chi$, and we are frequently considering the integral

$$I = \int y_0 P(\chi)\,d\chi \tag{57}$$

where $P(\chi)$ is a polynomial in χ. Then, by integration by parts,

$$I = y_0\left[P(\chi) - P'(\chi) + P''(\chi) - P'''(\chi) + \ldots\right] \tag{58}$$

In general, integrals of the form $I_m = \int {y_0}^m P(\chi)\,d\chi$, with $y_0 = e^{\chi}$, $P(\chi)$ a polynomial in χ and m a positive integer, will typically lead to I_m being expressed by a linear combination of $P(\chi)$ and its successive derivatives in the form of

$$\begin{aligned} I_m = {y_0}^m\big[&a_0 P(\chi) - a_1 P'(\chi) \\ &+ a_2 P''(\chi) - a_3 P'''(\chi) + a_4 P^{(IV)}(\chi) - \ldots\big] \end{aligned}$$

where the a_i are positive and depend on m.

Now, using χ as the independent variable, we are ready to start the derivation of the second-order solution. — From Eqs. (47c) and (52b),

$$\frac{d\phi_1}{d\chi} = \frac{1}{c}v_0 = \frac{1}{c^2}y_0 - \frac{1}{c^2} - \frac{k}{c}\chi \tag{59}$$

so that

$$\phi_1 = \frac{1}{c^2}\left(y_0 - 1\right) - \frac{1}{c^2}\chi - \frac{k}{2c}\chi^2 \tag{60}$$

With this into (55),

$$\frac{dz_1}{d\chi}=\frac{1}{c}\phi_1=\frac{1}{c^3}y_0-\frac{1}{c^3}-\frac{1}{c^3}\chi-\frac{k}{2c^2}\chi^2 \qquad (61)$$

which, with the initial condition $z_1(0)=0$, yields

$$z_1=\frac{1}{c^3}(y_0-1)-\frac{1}{c^3}\chi-\frac{1}{2c^3}\chi^2-\frac{k}{6c^2}\chi^3 \qquad (62)$$

and therefore, by (40),

$$y_1=\frac{1}{c^3}y_0\left[(y_0-1)-\chi-\frac{1}{2}\chi^2-\frac{kc}{6}\chi^3\right] \qquad (63)$$

Finally, for v_1, we consider Eq. (47b) transformed by (49) and (50):

$$\frac{dv_1}{d\chi}=\frac{1}{c}y_1-kv_0-\frac{k}{c}\phi_1 \qquad (64)$$

so that

$$\begin{aligned}v_1=&\frac{1}{c^4}\int {y_0}^2 d\chi\\&-\frac{1}{c^4}\int y_0\left(1+\chi+\frac{1}{2}\chi^2+\frac{kc}{6}\chi^3\right)d\chi\\&-k\int v_0 d\chi-\frac{k}{c}\int\phi_1 d\chi\end{aligned} \qquad (65)$$

Notice that

$$\int {y_0}^2 d\chi=\int y_0 dy_0=\frac{1}{2}{y_0}^2$$

$$\int v_0 d\chi=c\phi_1$$

$$\frac{1}{c}\int\phi_1 d\chi=z_1$$

whereas integrals of the form $I=\int y_0 P(\chi)d\chi$ are computed by Eq. (58). With these considerations, Eq. (65) leads, in final form, to

$$\begin{aligned}v_1=&\frac{1}{2c^4}(y_0-1)\left[y_0-1-2kc^3\right]\\&-\frac{1}{c^4}y_0\chi\left[kc+\frac{1}{2}(1-kc)\chi+\frac{kc}{6}\chi^2\right]\\&+\frac{k}{c^3}\chi\left[1+c^2+\frac{1}{2}\left(1+kc^3\right)\chi+\frac{kc}{6}\chi^2\right]\end{aligned} \qquad (66)$$

Eqs. (60), (63) and (66) constitute the complete second-order analytic solution for entry trajectories in the circular case.

By proceeding in a similar manner, system (48) can also be analytically integrated to produce a third-order solution. Since

$$\phi_2=\frac{1}{c}\int\left(v_1+\frac{1}{2}{v_0}^2\right)d\chi \qquad (67)$$

it can be shown that the third-order analytic expression for the flight path angle is

$$\begin{aligned}\phi_2=&\frac{1}{4c^5}\left(1+c^2\right)\left({y_0}^2-1\right)-\frac{1}{c^5}\left(2-3kc+c^2\right)(y_0-1)\\&+\frac{1}{c^5}y_0\chi\left[\left(1-3kc-kc^3\right)-\frac{1}{2}(1-2kc)\chi-\frac{kc}{6}\chi^2\right]\\&+\frac{1}{2c^5}\chi\left[\left(1+c^2+2kc^3\right)+kc\left(1+2c^2\right)\chi\right.\\&\left.+\frac{kc}{3}\left(1+2kc^3\right)\chi^2+\frac{k^2c^2}{12}\chi^3\right]\end{aligned} \qquad (68)$$

Next, observing that Eqs. (55) and (56) imply

$$z_2=\frac{1}{2}{z_1}^2+\frac{1}{c}\int\phi_2 d\chi \qquad (69)$$

and once again making use of Eq. (40), we find that the third-order expression for the nondimensional altitude/density variable is

$$\begin{aligned}y_2=&\frac{1}{8c^6}\left(5+c^2\right){y_0}^2(y_0-1)\\&-\frac{1}{8c^6}\left(35-72kc+7c^2-8kc^3\right)y_0(y_0-1)\\&+\frac{1}{c^6}{y_0}^2\chi\left[\left(1-6kc-kc^3\right)-\left(1-\frac{3kc}{2}\right)\chi-\frac{kc}{3}\chi^2\right]\\&+\frac{1}{2c^6}y_0\chi\left[\left(\frac{11}{2}-6kc+\frac{3c^2}{2}\right)+\left(\frac{5}{2}+\frac{c^2}{2}+kc^3\right)\chi\right.\\&+\left(1+\frac{2kc}{3}+\frac{2kc^3}{3}\right)\chi^2+\left(\frac{1}{4}+\frac{5kc}{12}+\frac{k^2c^4}{6}\right)\chi^3\\&\left.+\frac{kc}{6}\left(1+\frac{kc}{10}\right)\chi^4+\frac{k^2c^2}{36}\chi^5\right]\end{aligned} \qquad (70)$$

Now, from Eq. (48b) we obtain

$$\frac{dv_2}{d\chi}=\frac{1}{c}y_2-k\left(v_1+\frac{1}{2}{v_0}^2\right)-\frac{k}{c}v_0\phi_1-\frac{k}{c}\phi_2 \qquad (71)$$

Integrating,

$$v_2 = \frac{1}{c}\int y_2 d\chi - kc\int \frac{1}{c}\left(v_1 + \frac{1}{2}v_0^2\right)d\chi - \frac{k}{c}\int v_0\phi_1 d\chi - \frac{k}{c}\int \phi_2 d\chi \tag{72}$$

which, in view of Eqs. (67) and (69), becomes

$$v_2 = \frac{1}{2}kz_1^2 - kz_2 - kc\phi_2 - \frac{k}{c}\int v_0\phi_1 d\chi + \frac{1}{c}\int y_2 d\chi \tag{73}$$

And, recognizing that

$$v_0 d\chi = cd\phi_1 \quad \Rightarrow \quad \frac{1}{c}\int v_0\phi_1 d\chi = \int \phi_1 d\phi_1 = \frac{1}{2}\phi_1^2$$

the third-order formula for the nondimensional speed variable becomes, in final form,

$$v_2 = \frac{k}{2}z_1^2 - kz_2 - kc\phi_2 - \frac{k}{2}\phi_1^2 + \frac{1}{c^7}I_{v_2}(\chi) \tag{74}$$

where

$$\begin{aligned} I_{v_2}(\chi) &= c^6\int y_2 d\chi \\ &= \frac{1}{24}\left(5+c^2\right)\left(y_0^3-1\right) \\ &\quad -\frac{1}{2}\left(6-13kc+c^2-\frac{3}{2}kc^3\right)\left(y_0^2-1\right) \\ &\quad +\frac{1}{8}\left(33-104kc+5c^2-16kc^3+72k^2c^2+16k^2c^4\right)\left(y_0-1\right) \\ &\qquad +\frac{1}{2}y_0^2\chi\left[\left(2-8kc-kc^3\right)-(1-2kc)\chi-\frac{kc}{3}\chi^2\right] \\ &\qquad +\frac{1}{2}y_0\chi\left[2\left(\frac{1}{4}+\frac{c^2}{4}+4kc+kc^3-9k^2c^2-2k^2c^4\right)\right. \\ &\qquad\quad \left.+\left(\frac{5}{2}+\frac{c^2}{2}-7kc-kc^3+9k^2c^2+2k^2c^4\right)\chi\right. \\ &\qquad\quad +\frac{kc}{3}\left(7+2c^2-9kc-2kc^3\right)\chi^2 \\ &\qquad\quad +\left(\frac{1}{4}-\frac{5kc}{12}+\frac{3k^2c^2}{4}+\frac{k^2c^4}{6}\right)\chi^3 \\ &\qquad\quad \left.+\frac{kc}{6}\left(1-\frac{9kc}{10}\right)\chi^4+\frac{k^2c^2}{36}\chi^5\right] \end{aligned} \tag{75}$$

Eqs. (68), (70), (74) and (75) represent the complete third-order analytic solution for entry trajectories in the circular case. — The various orders of solutions are compared in Figs. 9-12.

Entry at circular speed displays a somewhat different behavior than the subcircular case. While the altitude follows the same general trend as before, the flight path angle does not. No steep initial variation of γ is observed. Instead, it varies quite slowly through the first two thirds of the trajectory. Only towards the end of the entry does the rate of variation of γ increase significantly. A similar behavior is noticed in the speed. On the other hand, the deceleration displays very much the same trend as in the subcircular case. Although the analytic solutions for the circular case are quite different than the non-circular cases, comparison of the various solutions again shows very clearly that the higher the order, the greater the accuracy, with the third-order yielding indeed very good results. Also, like the subcircular case, it is noted that, as $|\gamma_e|$ increases, the agreement between analytic and numerical solutions improves. Once again, while the results for altitude, speed, and deceleration are excellent, those for γ are only moderate. A fourth-order solution might, in theory, have the potential to solve the problem.

Conclusions

A new set of higher-order analytic solutions has been obtained for three critical classes of maneuvers, viz., ballistic skip at supercircular speed, shallow ballistic entry at subcircular speed, and shallow ballistic entry from low circular orbits.

Starting with the equations of motion for planar entry into a non-rotating, spherical planetary atmosphere, we have used normalization to put the equations in a form adequate for integration via analytic continuation.

The solutions obtained have been shown to be very accurate and fast, being suitable for guidance purposes as well as mission planning and stability analysis. Explicit relationships between altitude, speed, flight path angle, and distance traveled are provided.

References

[1]Chapman, D.R., "An Approximate Analytical Method for Studying Entry into Planetary Atmospheres," *NASA TR R-11*, Washington, DC, 1959.

[2]Loh, W.H.T., *Dynamics and Thermodynamics of Planetary Entry*, Prentice-Hall, Englewood Cliffs, NJ, 1963.

[3]Yaroshevskii, V.A., "The Approximate Calculation of Trajectories of Entry Into the Atmosphere. I," translated from *Kosmicheskie Issledovaniya*, Vol. 2, No. 4, 1964.

[4]Longuski, J.M., and Vinh, N.X., "Analytic Theory of Orbit Contraction and Ballistic Entry into Planetary Atmospheres," *JPL Publication 80-58*, Pasadena, CA, 1980.

[5]Vinh, N.X., Kim, E.-K., and Greenwood, D.T., "Second-Order Analytic Solutions for Re-Entry Trajectories," Paper No. AIAA 93-3679, AIAA Atmospheric Flight Mechanics Conference, Monterey, CA, 1993.

[6]Abramowitz, M. & Stegun, I., *Handbook of Mathematical Functions with Formulas, Graphs, and*

Mathematical Tables, US Government Printing Office, Washington, DC, 1964.

[7]Salzer, H.E., "Formulas for Calculating the Error Function of a Complex Variable," *Mathematical Tables and Aids to Computation*, Vol. 5, pp. 67-70, 1951.

Figures

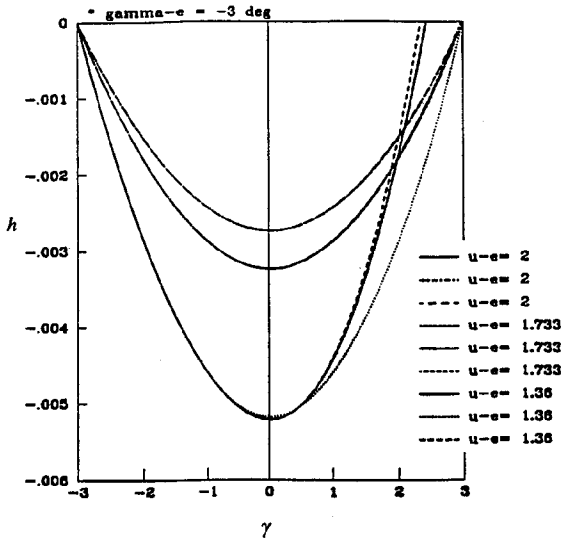

Fig. 2 - Variation of the altitude during ballistic skip at supercircular speed ($\gamma_e = -3°$).

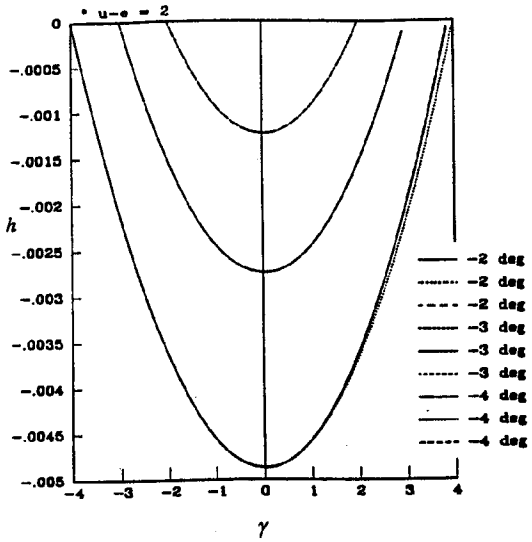

Fig. 4 - Variation of the altitude during ballistic skip at supercircular speed ($u_e = 2$).

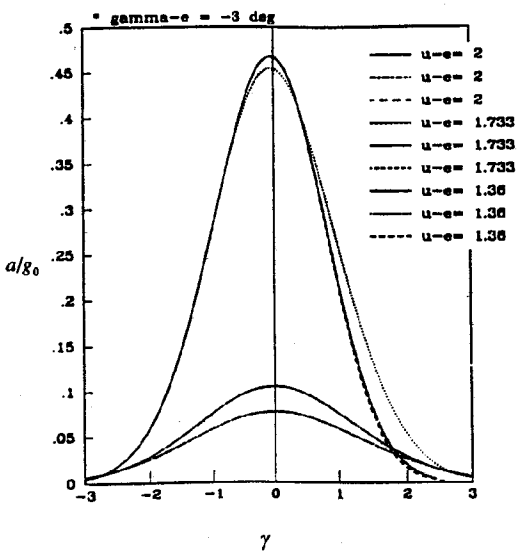

Fig. 3 - Deceleration due to drag during ballistic skip at supercircular speed ($\gamma_e = -3°$).

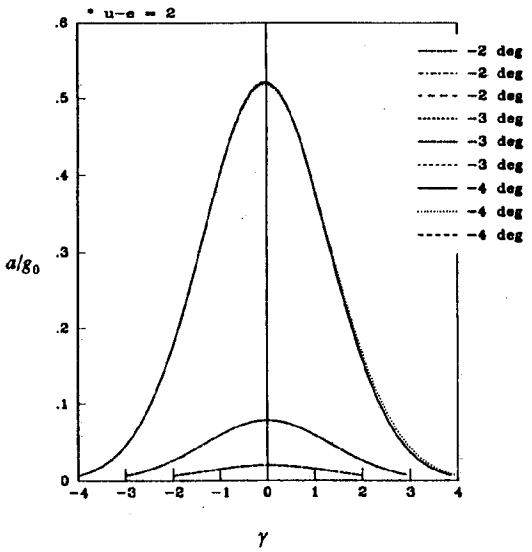

Fig. 5 - Deceleration due to drag during ballistic skip at supercircular speed ($u_e = 2$).

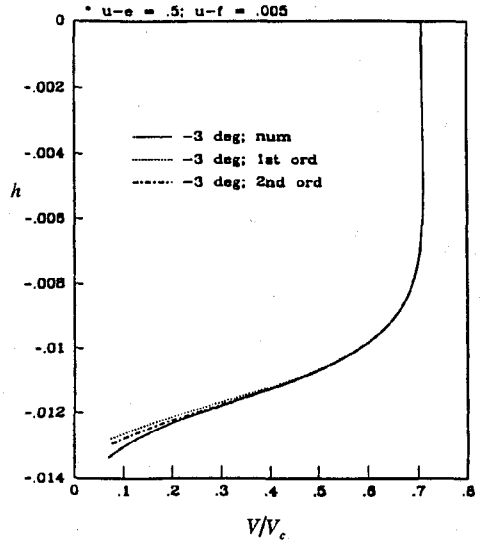

Fig. 6 - Variation of the altitude during ballistic entry at subcircular speed ($u_e = 0.5$).

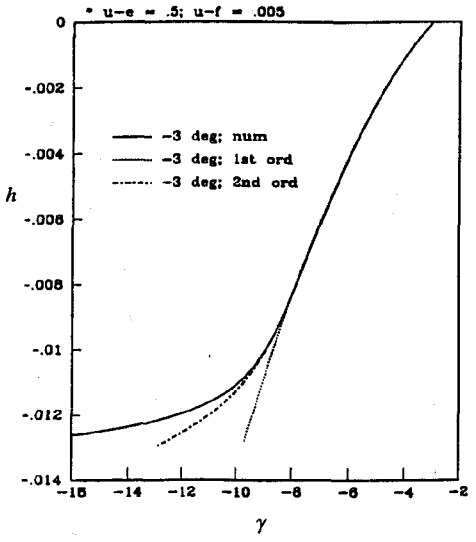

Fig. 8 - Variation of the altitude for ballistic entry at subcircular speed ($u_e = 0.5$).

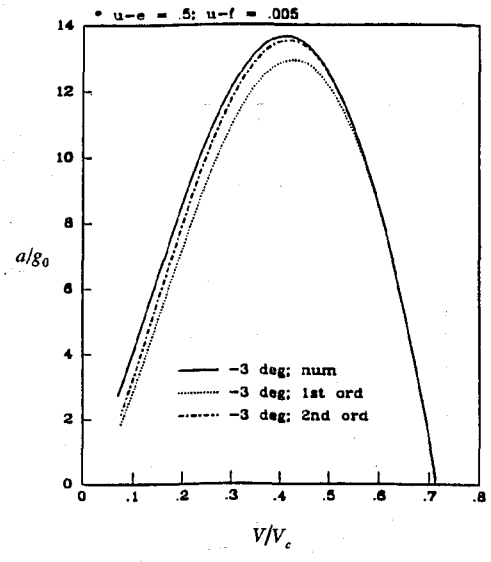

Fig. 7 - Deceleration due to drag during ballistic entry at subcircular speed ($u_e = 0.5$).

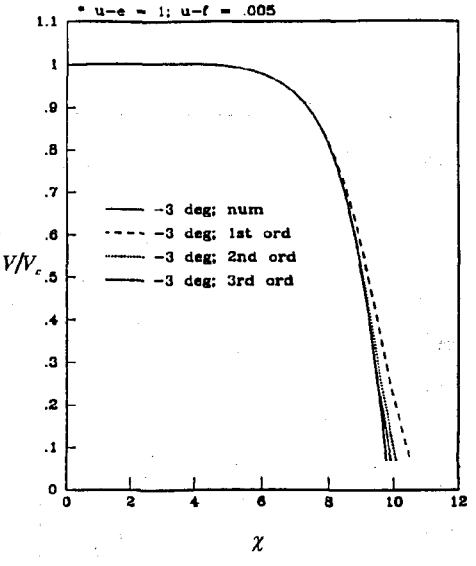

Fig. 9 - Speed-longitude profile in ballistic entry at circular speed.

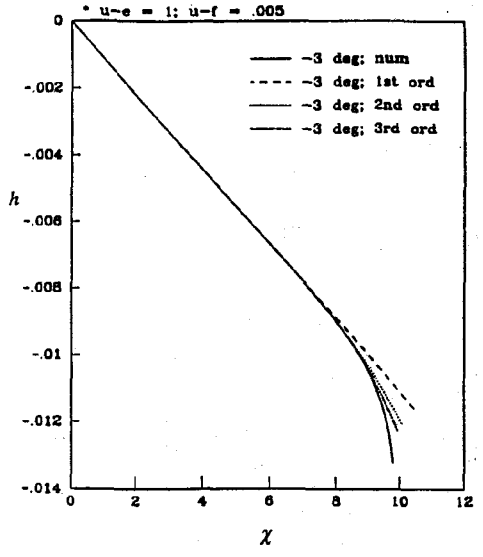

Fig. 10 - Altitude-longitude profile in ballistic entry at circular speed.

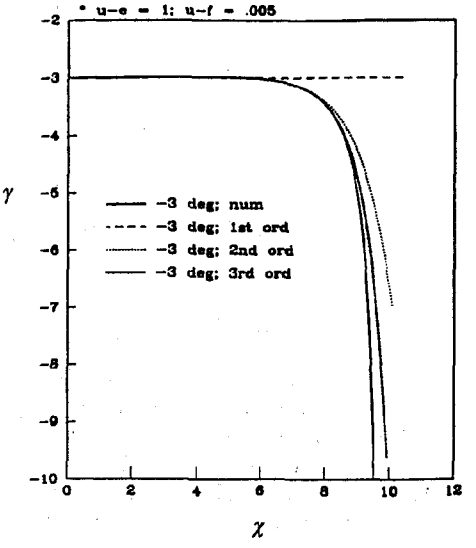

Fig. 12 - Flight path angle versus transformed longitude in ballistic entry at circular speed.

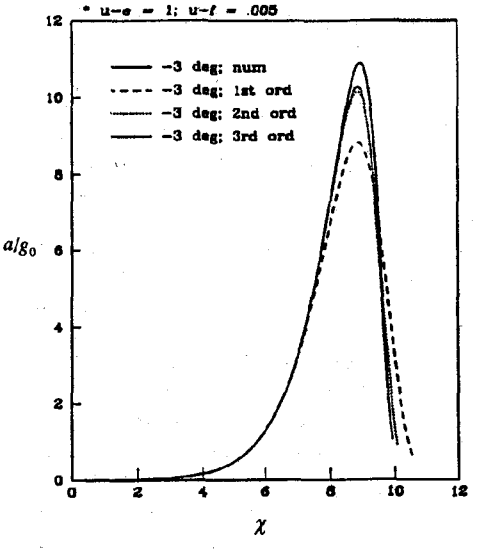

Fig. 11 - Deceleration-longitude profile in ballistic entry at circular speed.